How long to oceanic tracer and proxy equilibrium?

Carl Wunsch*, Patrick Heimbach

Department of Earth, Atmospheric and Planetary Sciences, Massachusetts Institute of Technology, Cambridge, MA 02139, USA

Abstract

The various time scales for distribution of tracers and proxies in the global ocean are critical to the interpretation of data from deep-sea cores. To obtain some basic physical insight into their behavior, a global ocean circulation model, forced to least-square consistency with modern data, is used to find lower bounds for the time taken by surface-injected passive tracers to reach equilibrium. Depending upon the geographical scope of the injection, major gradients exist, laterally, between the abyssal North Atlantic and North Pacific, and vertically over much of the ocean, persisting for periods longer than 2000 years and with magnitudes bearing little or no relation to radiocarbon ages. The relative vigor of the North Atlantic convective process means that tracer events originating far from that location at the sea surface will tend to display abyssal signatures there first, possibly leading to misinterpretation of the event location. Ice volume (glacio-eustatic) corrections to deep-sea $\delta^{18}O$ values, involving fresh water addition or subtraction, regionally at the sea surface, cannot be assumed to be close to instantaneous in the global ocean, and must be determined quantitatively by modelling the flow and by including numerous more complex dynamical interactions.

© 2008 Elsevier Ltd. All rights reserved.

1. Introduction

A great deal of paleoceanographic inference depends directly upon the distribution of proxies, in the form of passive tracers, as observed throughout the global ocean. Examples are $\delta^{18}O$, $\delta^{13}C$, and ^{14}C. Often the distributions measured in cores are interpreted as depicting a system at tracer equilibrium—in the specific sense that the system has become globally uniform and, as also unchanging over extended periods. A globally uniform steady-state can be far easier to interpret than one undergoing transient changes or retaining spatial gradients, and it is important to understand just how long it does take for the ocean to produce both uniformity and a nearly unchanging state.

The inference is widespread (a recent example is Skinner and Shackleton, 2005) that horizontally uniform tracer distributions are reached after circa 1000 years. These authors attribute to Duplessy et al. (1991) the estimate that

the time scale for propagation of signals from the North Atlantic to the North Pacific cannot exceed about 1500 years—an inference based upon radiocarbon ages. They rationalize an observed lag of about 4000 years between the two ocean basins in their core data primarily in terms of regional hydrographic changes. Undoubtedly, such changes exist in a system as complex as the ocean. But as we will discuss here, there may be an even simpler explanation for what is observed: the results suggest that times to uniformity greatly exceed 1500 years even when the circulation is steady.

Key et al. (2004) (see Sarmiento and Gruber, 2006, Fig. 2.4.2) show that radiocarbon ages in the deep (3500 m) North Atlantic are about 700 years and in the deep North Pacific are a bit over 2000 years, roughly consistent with the Duplessy et al. (1991) and other such estimates. If one divides the volume of the world ocean (about $3 \times 10^{18} \, \mathrm{m}^3$) by a deep water production rate of 20 Sv, a reservoir time of about 2000 years is obtained. The idea of a tracer age as the time to equilibrium, and the reassuring rough consistency of the radiocarbon age with the reservoir time, seems to underlie the general sense in the paleo-literature that changes taking place over time scales of about 2000

*Corresponding author. Tel.: +1 617 253 5937; fax: +1 617 253 4464.

E-mail addresses: cwunsch@mit.edu (C. Wunsch), heimbach@mit.edu (P. Heimbach).

years and longer permit discussion of spatial equilibrium tracer distributions.[1]

Reservoir times, however, only provide a gross order of magnitude—they do not address the possibility that major parts of the ocean are much more rapidly ventilated than others, thus producing long-lived tracer gradients and hence tracer signals in the sediments. Tracer ages are, moreover, extremely difficult to interpret. Although it seems not widely recognized, a number of papers (e.g., Haine and Hall, 2002; Wunsch, 2002; Waugh et al., 2003) have shown that tracer ages are functions of the tracer properties including, particularly, the radioactive decay constants. Appendix B provides a simple analytical example, using the Munk abyssal recipes vertical balance, to demonstrate that the tracer age can vary by several orders of magnitude depending upon which particular tracer is used. Some more general comments are made there concerning three-dimensional solution asymptotics.

Many time scales are present in a fluid flow as complex as the ocean circulation, because signals and changes can be carried by a wide variety of physical mechanisms, from boundary-trapped waves to large-scale diffusion. Of special importance are signalling times—when a remote observer might be able to infer that something had happened elsewhere, the very different time at which the whole system has come into a new steady-state, "ventilation times" and other definitions. These various time scales can differ by orders of magnitude, but here the focus is on how large-scale, long-duration, tracer changes in the ocean might be recorded in the sediments, with implications for calculations such as that of Skinner and Shackleton (2005).

The results are reported of some simple experiments with a near-global oceanic general circulation model, using passive tracer distributions to estimate the times required for the global ocean to reach a uniform tracer distribution. For the specific experiments described below, time-to-uniformity is identical to the time-to-tracer-equilibrium. Many of these results are already available, at least implicitly, in a number of published calculations reporting "transit-time" and related distributions in the ocean (e.g., Khatiwala et al., 2005; Waugh et al., 2003; Peacock and Maltrud, 2006; Primeau and Holzer, 2006), which are calculations of oceanic boundary Green functions—responses to imposed surface transients resembling delta functions. These computations demonstrate the variety of scales, in particular the very long ones, present in large-scale oceanic tracer distributions. But the implications seem not widely known to the paleo-community, and the major purpose here is not to dismiss the transient time distributions, but rather to render them in a more simple, concrete, fashion.

Many different calculations can be done for timescale determination. Define here what may be the simplest of all tracer experiments—a special case directed simultaneously at the time to uniformity, and to equilibrium—where the basic flow patterns are not themselves subject to significant low frequency variability, and in particular, are not affected by the tracer distributions. The latter assumption is a major simplification, e.g., of the problem of tracer signatures coupled to fresh water transfers or thermal disturbances; passive and active tracers will not generally follow the same pathways, and with the latter changing the flow field.

This paper reports an exercise in geophysical fluid dynamics—the model is believed to capture the dominant physical processes of the ocean circulation and of tracer movement, but it is not (and cannot) be fully realistic in representing the ocean circulation over any 2000+ year interval. Basic insight is sought, not detailed realism.

2. The circulation employed

The ocean circulation studied is that of *the present-day*, as estimated by using a 1° horizontal resolution, 23-vertical layer model with a 1 h time-step as described by Wunsch and Heimbach (2006, 2007). This so-called ECCO-GOD-AE (Estimating the Circulation and Climate of the Ocean—Global Ocean Data Assimilation Experiment) model has been adjusted by least-square methods to nearly full consistency over 13 years to the global ocean observations available in the interval 1992–2004. The underlying numerical code is that of Marshall et al. (1997) as modified by the ECCO projects in the interim, and includes the Large et al. (1994) mixed layer formulation, and the Gent and McWilliams (1990) eddy-flux parameterization. Results are shown using the model running freely (unconstrained) with the adjusted initial and boundary conditions so as to pass within error bars of approximately 100 million ocean observations and about 2 billion atmospheric estimates, all weighted according to their estimated errors during 1992–2004. No tracer data, other than temperature and salinity, were used in determining the circulation. Having the model run free means that the solutions are consistent with the numerical equations of the model, with no artificial jumps or inconsistencies introduced by some other data-constraint schemes.

The specific solution used here is from an experimental ECCO-GODAE version 3 configuration. Appendix A describes the major changes from the version 2 solutions of Wunsch and Heimbach (2007). Comparisons with tracer calculations made with version 2 solutions will be touched on later.

A 50-year perpetual loop covering the NCEP/NCAR reanalysis period 1955–2005 is constructed from the adjusted atmospheric state of the 13-year version 3 solution (Appendix A). Thus the flow field in the system evolves very slowly over the almost-2000 year calculation. No one

---

[1]Numbers calculated by Huang (1999) suggest that the entire volume of the ocean transits the mid-ocean ridges in the hydrothermal cycle at a rate of about 12 Sv, for a reservoir time of about 3000 years. This interesting potential complication is not further addressed here.

expects the circulation to remain fixed over thousands of years or to have a near-periodic perturbation in the fashion described in Appendix A. Nonetheless, in this form, the circulation is as realistic a representation of the modern world as we can make it, captures the very strong annual cycle and interannual variability in some regions, and should maintain the statistics of the decadal variability even as the system would slowly change. Major unknown changes in the oceanic past (and future) would introduce many additional new time scales into the problem, and they must be studied separately. The near-periodic forcing leads to a 25–50 year "chatter" or noise in the concentration trends at points, which seems to be of little importance, because tracer distributions integrate through small-scale space and time structures, tending to suppress them, except in a few areas where an extrapolation explained later can be rendered unstable.

The pathways by which tracers move through the global ocean are extremely complex, three-dimensional, and time-evolving. Tracers can reach any particular location through multiple pathways in both space and time (e.g., consider any location involving a mixture of Circumpolar and North Atlantic Deep Water, where pathways and mixing can change with the seasons and longer times). Depiction of all of these pathways and their time histories would comprise a complete description of the three-dimensional time-dependent ocean circulation, an undertaking far beyond our present ambitions. Thus most of the detail obtained in the tracer movements through the model ocean is being suppressed in favor of a determination of bulk time scales. The expected long-time variations in the ocean circulation, and those present in the model, are likely to delay equilibria, not accelerate it.

3. The tracer experiments

Because running a global dynamical model to full equilibrium even with a resolution as coarse as $1°$ is still computationally expensive, we carry out 12 simultaneous tracer experiments in which the final equilibrium, not fully achieved because it is an asymptotic process, is known in advance. Conceptually, we dye the sea surface some color, perhaps red, with concentration $C_0 = 1$, over a finite ocean area or the entire ocean starting at $t = 0$, and maintain that surface tracer concentration forever afterwards. In regions where no dye is introduced, a no-flux boundary condition is used to prevent the dye from being exchanged with the atmosphere. Here the "dye" is completely passive, having no dynamical, chemical, or biological interactions and the color is just notional. In such a system, the final steady-state is known, and is $C = C_0$, everywhere. Thus equilibrium and uniformity coincide here, and we will use the terms interchangeably. The time required to come within some small distance, Δ, of the equilibrium will be a function of the surface distribution and observation location within the three-dimensional ocean. Other boundary conditions (e.g., ones forcing zero surface concentration

in areas of no dye) permit fluxes of dye to the atmosphere, and the final equilibrium, $C \leqslant 1$, would be a function of position, and which it would be necessary to compute.

Other boundary conditions, e.g., a fixed flux through the surface everywhere, will give different results. Globally uniform flux into the ocean can be expected to produce shorter time scales than will be seen here, as extremely large gradients *within* the ocean can then build up. Whether any real tracer is best represented that way is somewhat doubtful. Ultimately, as in so many aspects of climate, the coupled ocean-atmosphere must be considered as a single system (and for some purposes terrestrial and cryospheric reservoirs must be included as well). To reiterate, we are not providing a general result—only a simple computation intended primarily as a scale analysis.

As will be seen, in some of the experiments, particularly those for regional inputs, even the nearly 2000 years of integration remains far short of achieving near-uniformity over much of the ocean. "Practical equilibrium" will be defined here as the time, t_{90}, where the concentration evolution reaches $0.9C_0$—90% of the final value; that is, $\Delta = 0.1$. This definition of a time-scale has the virtue of a very simple physical interpretation. Fuller uniformity (e.g., 99%) will normally take a good deal longer. Anyone trying to interpret actual proxy or tracer data would need to decide how large a deviation from the final value can be tolerated—there is no universal answer. Some of the various injection domains are shown in Fig. 1.

For discussion of the details of the flow field we must refer the reader elsewhere (Wunsch and Heimbach, 2006, 2007). Note only that there is some evidence (F. Schott, personal communication, 2007) that the model produces overly energetic convection in the high latitude North Atlantic. It is generally believed (R. Ferrari, personal communication, 2007) that such effects, common in models, arise from the coarse $1°$ horizontal resolution, and inadequately parameterized horizontal eddy fluxes. In particular, restratification after winter-time convection is too slow, permitting subsequent winter convection events to reach too deep. Such effects will tend to produce model equilibrium times that are *lower bounds*.

On the other hand, the model, in common with essentially all ocean general circulation models, does not properly produce Antarctic Bottom Water (AABW)—a process dependent upon the detailed representation of a range of small scale processes on the Antarctic continental margin, including ice shelves, as well as interactions there with sea ice. To the degree that tracer injection occurs through AABW formation, it is not correctly present here, and we will likely overestimate the time to equilibrium from this particular injection process, proportional to the fraction of bottom water made near Antarctica, although reduced tracer transfer from the atmosphere through perennially ice-covered regions will mitigate the effect.

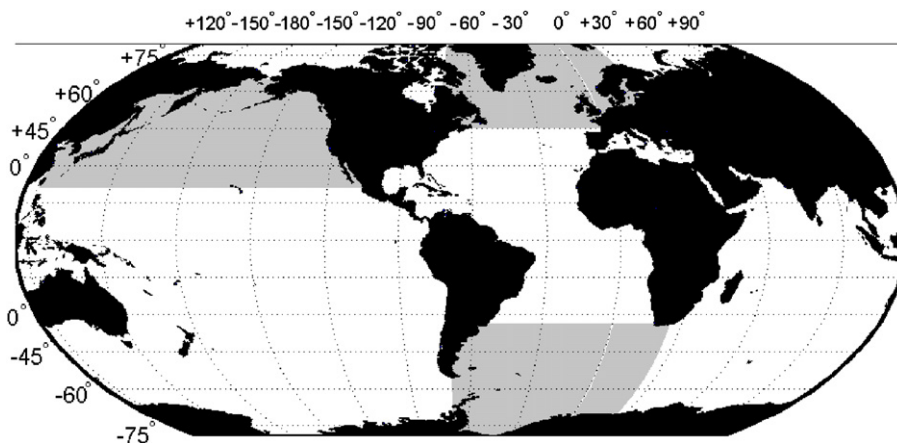We discuss some of these experiments in turn, starting with the global one.

Fig. 1. Three of the regions, in addition to the global one, for tracer inputs discussed here. The "color" injected in each region is different, although all are shown here as gray. Results were obtained for a total of 12 regions (including the global one), but only the ones depicted are discussed here. Other regions consist of the North Atlantic (20–80°N); tropical Atlantic; South Atlantic; tropical Pacific (20°S–20°N); Indian Ocean; Indian sector of the Southern Ocean; and Pacific sector of the Southern Ocean with results available from the authors.
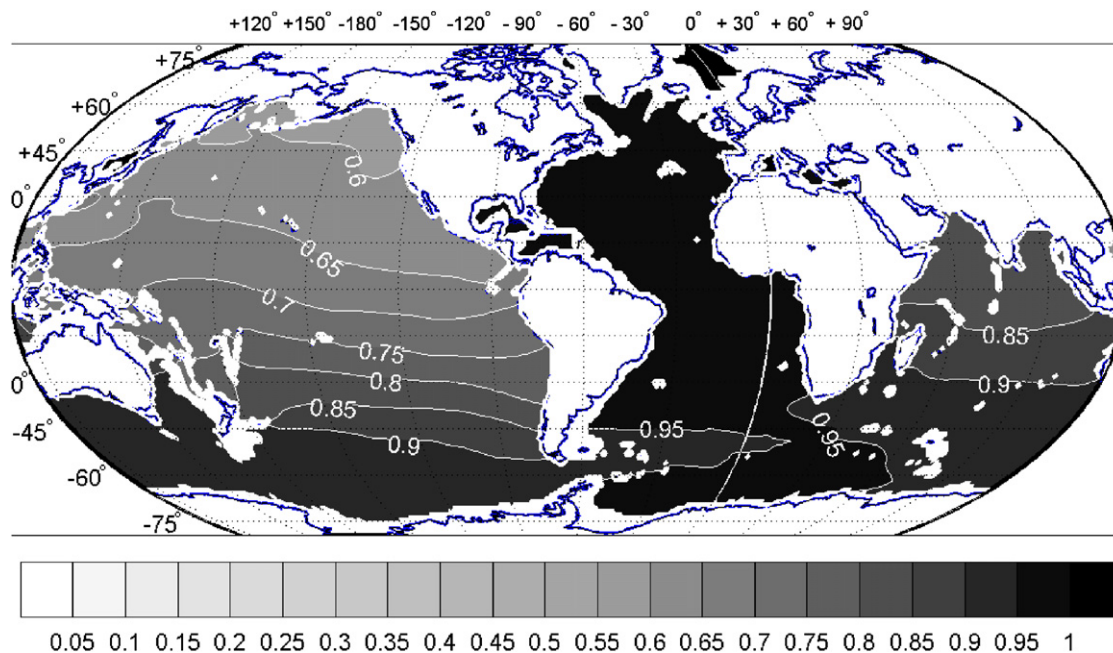
Fig. 2. Concentration at 1975 m after 1900 years from a globally uniform surface dye distribution. Ultimate equilibrium concentration is $C = 1$ everywhere. The North Atlantic to North Pacific gradient is very strong even after such a long time. Isolated regions of zero concentration are typically topographic features shallower than the reference depth being used.

3.1. Experiment 1. Global coverage

In the first experiment, the entire ocean, which is initially entirely free of tracer, is given uniform surface concentration $C = C_0 = 1$, starting at $t = 0$; this experiment is the simplest one of interest. Fig. 2 shows the concentration in the middle of the layer at 1975 m after 1900 years. To a large degree, this figure already shows the major results of this paper: although the abyssal Atlantic and Southern Oceans are within a very small distance of their final tracer value, the mid-depth Pacific is still at only 70% or less of the asymptote. Bottom dwelling organisms alive at this

time, able to record the signal, would depict strong spatial gradients between ocean basins. A somewhat different view is seen in Fig. 3 showing the latitude–depth concentrations down the middle of the Pacific Ocean at the same time.

The North Atlantic is the site of highly active convection over a comparatively confined region, and leading to excessive concentrations there at depth. High latitude intermediate depth convection also occurs in the Southern Ocean, but spread over a much wider area and thus producing concentrations small compared to similar depths in the North Atlantic, but with similar or larger total tracer inventories.
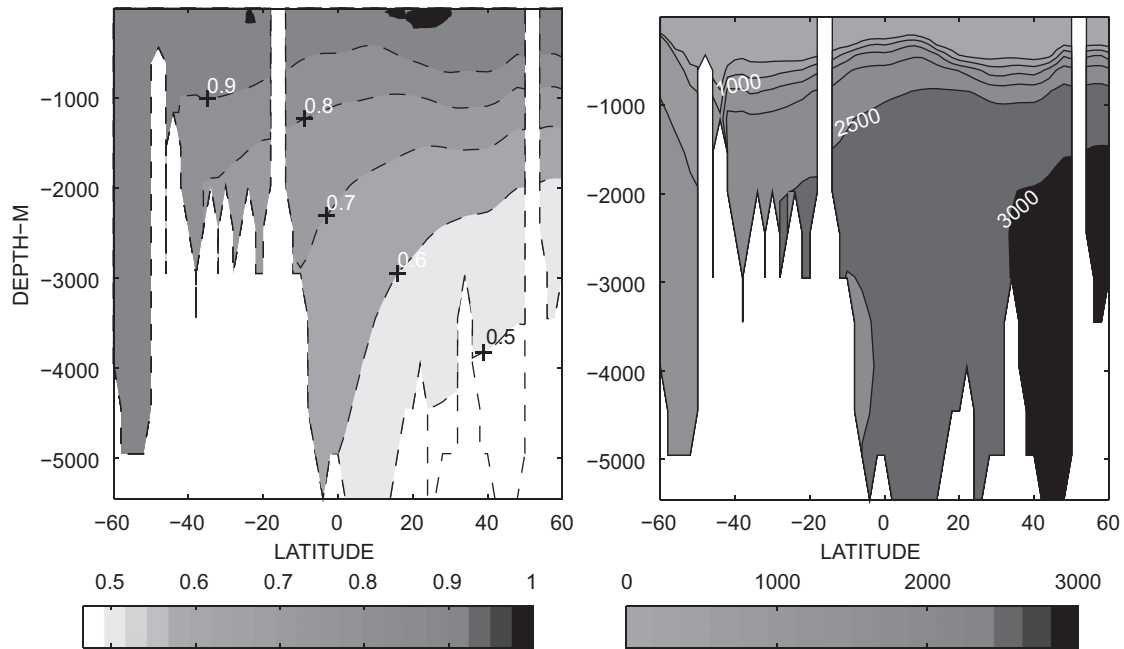
Fig. 3. Meridional section down 180° longitude displaying (left panel) the gradual reduction in tracer concentration with latitude after 2000 years and in the right panel the estimated value of t_{90} in years.

One would like a quantitative estimate of the time to the final uniform steady-state, a computation complicated by our inability to run the system completely to the final value of $C = 1$ everywhere. To proceed, it is helpful to gain some understanding of the way in which equilibrium is achieved, anticipating that because tracer evolution at any given location is the end result of a three-dimensional time-evolution of the solution to an equation such as

$$\frac{\partial C}{\partial t} + \mathbf{v} \cdot \nabla C - \nabla(\mathbf{K}\nabla C) = 0, \qquad (1)$$

subject to boundary and initial conditions, where $\mathbf{K}$ is a mixing tensor and the operators and velocity field, $\mathbf{v}$, are three-dimensional. In a complex geometry and flow field, the solutions to C are not expected to display any simple globally applicable behavior. Nonetheless (cf. Peacock and Maltrud, 2006), one can hope for some rules of thumb useful in obtaining orders of magnitude. Figs. 4 and 5 display the time histories at 1975 m along two longitude lines down the Atlantic and Pacific Oceans. The asymptotic nature of equilibrium is clear. A nearly linear initial rise followed by a continued slower, asymptoting, exponential growth toward $C = 1$ can be seen (some one-dimensional transient analytical solutions exhibit such behavior; see Appendix B). In the North Pacific, in particular, where 1900 years is still significantly short of the equilibrium time, the time histories are still in the linear phase at the end of the computation. (Some regions show a brief, steeper, linear rise, immediately after finite tracer concentration onset that seems related to a very rapid, mainly advective, arrival.) To obtain a lower bound on the time to uniformity in regions still undergoing rapid rise, we use t_{90}. Where the maximum $C < 0.9$, a linear extrapolation for t_{90}, based
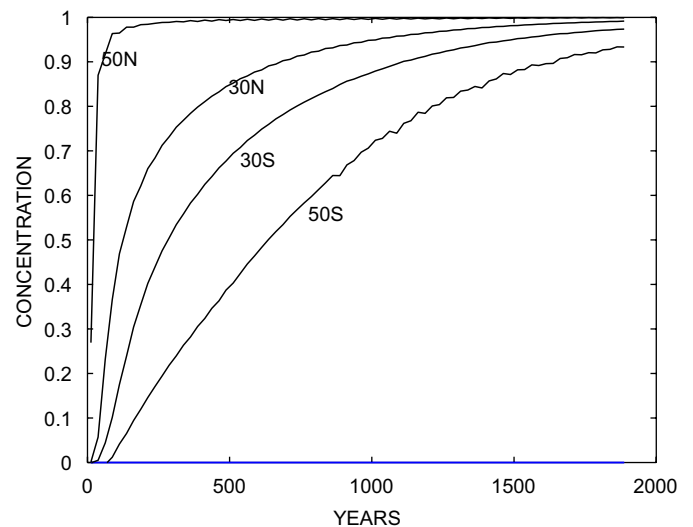

Fig. 4. Time series of tracer conservation at 1975 m along 30 W at several latitudes in the Atlantic Ocean in the global injection experiment. Some of the chatter owing to the cycling nature of the forcing is visible in the plots.

upon the last 200 years of history (and smoothed as a 250-year running average), is used. Evidently, given the shapes of the temporal curves, such an extrapolation will produce a time that *underestimates*, sometimes greatly, the true value of t_{90} at those locations (that is, the extrapolation does not capture the strong reduction in the asymptotic rate of rise).[2]

---

[2]Note that signalling times—when a local observer could determine that tracer had first arrived—would depend directly upon his detection threshold.

Fig. 6 displays the estimated value of t_{90} at 1975 m. The times to achieve t_{90} in the North Pacific Ocean are all significantly greater than 2000 years. Values near 1000 years in the subtropical Atlantic are roughly consistent with the estimate obtained from a simple box model by Wunsch (2003) and with the independent transit-time calculations. Note the considerable zonal structure in the Southern Ocean—time-scales-to-equilibrium depend strongly upon longitude and expectations of zonal homogeneity would be difficult to sustain except on much longer durations.

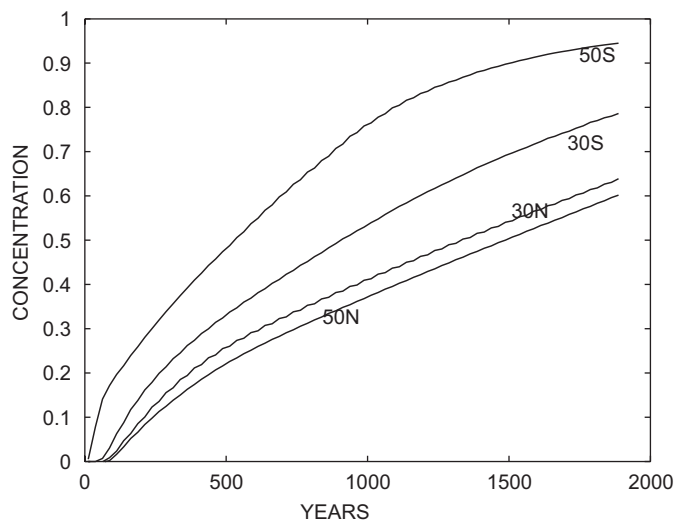Near-surface values in this global injection experiment achieve uniformity almost immediately, while abyssal values undergo several thousand years of evolution and arrive along many different fluid pathways from all possible surface positions. Fig. 7 shows the estimated t_{90} at 3950 m. Some of the longest estimated times are now in the western tropical Pacific as well as the far northern Pacific regions. The concentration and t_{90} patterns are similar as expected, but differ in detail.

As noted above, there is no proper representation of AABW production in a 1° horizontal 23-layer model and so that injection to the very abyss is not properly represented here, with the North Atlantic region dominating the dye concentration of the deepest model layers. The inventory at mid-depths is, nonetheless, largely in the Southern Ocean, with approximately 40% of the dye below 1000 m lying south of about 35°S at all times shorter than 500 years. Fig. 8 shows the zonally summed deep tracer concentration (below 1000 m) at 500 years weighted by the layer thickness and latitude. The very small region of the North Atlantic, which visually, dominates latitude–longitude contour patterns, is approximately compensated by the much larger area occupied by the Southern Ocean.

3.2. North Atlantic high latitude injection

The global experiment produces the shortest values of t_{90} by virtue of having the largest possible area of tracer input. Injections restricted to any subregion will necessarily take much longer to reach global near-equilibrium. The high latitude North Atlantic (Fig. 1) is of particular interest both because it has the most rapid communication with the abyss, and because it would be one of the major regions of injection of glacial ice water melt, producing anomalous $\delta^{18}O$, among other tracers. Fig. 9 shows the surface concentrations after 2000 years. Because the tracer is carried solely by the ocean circulation and not by the atmosphere, most of the surface dye field is still confined to
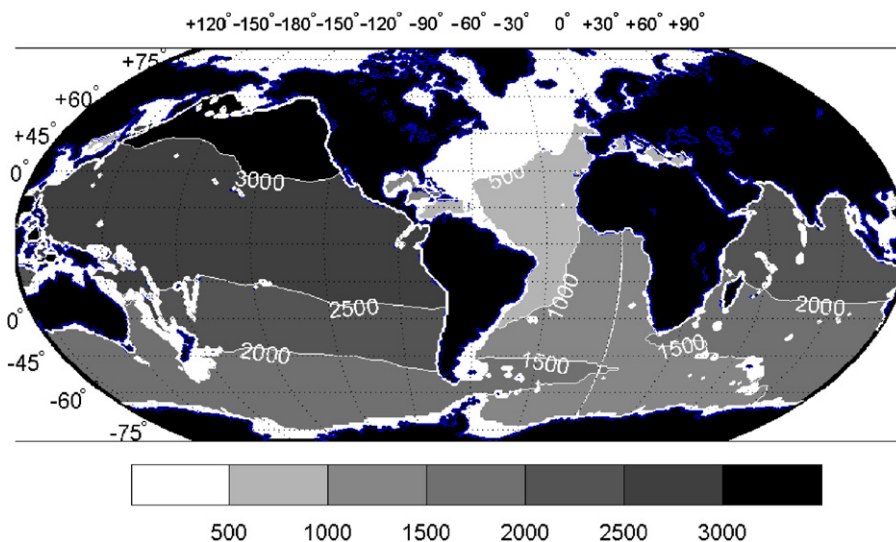

Fig. 5. Same as Fig. 4 except along 180 W in the Pacific. The initial rapid linear increase at 50°S likely the reflects the fast zonal advection within the Southern Ocean. Note that the northern Pacific curves are still rising rapidly, in a nearly linear phase, and have not yet reached the asymptotic transition.

Fig. 6. Time, t_{90}, at which the globally input tracer achieves 90% of its equilibrium value at 1975 m. Values exceeding 2000 years are from extrapolation and are a lower bound on the true value. As with the concentration charts, isolated regions with $t_{90} = 0$ are below the bottom topography of the model.
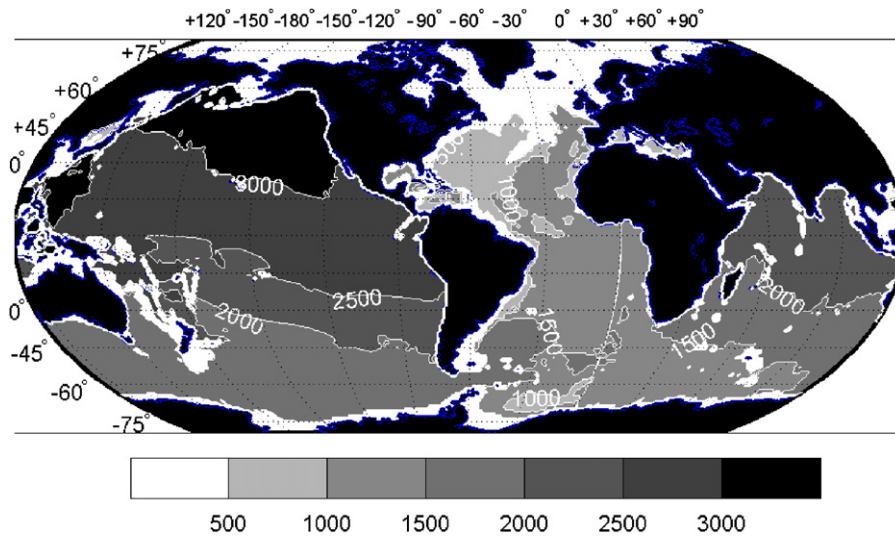
Fig. 7. Same as Fig. 6 except at 3950 m. Note the measurable gradients persisting in the deep Southern Ocean.
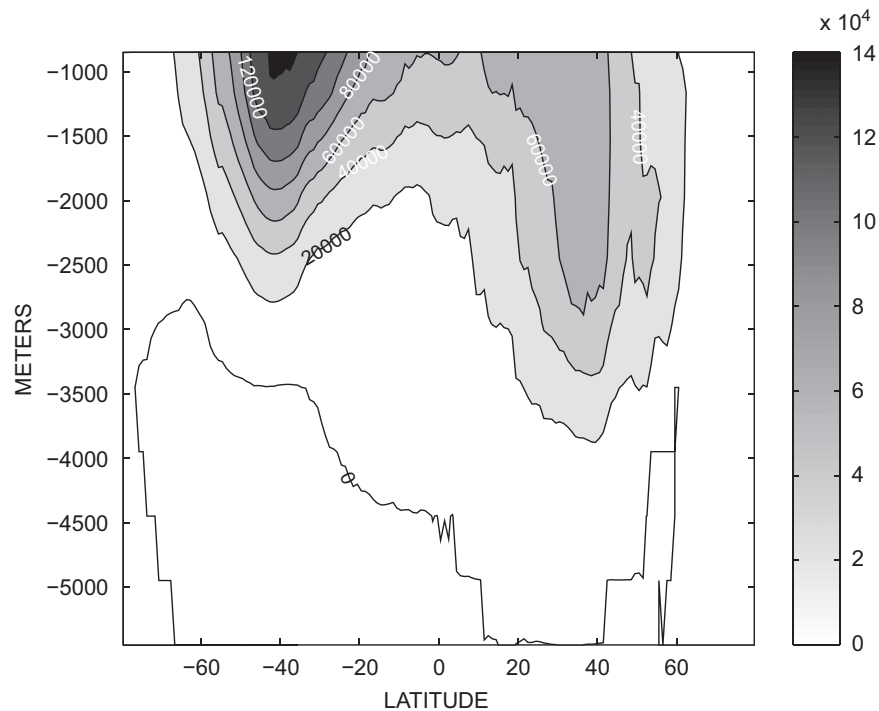

Fig. 8. Zonal sum of the tracer concentration weighted by the layer thickness and latitude (units of tracer times meters) after 500 years in the global experiment. Note that the depths all lie below 1000 m.

the northern North Atlantic, although finite amounts are found everywhere. (Injected ice-melt has a dynamical signature as well as a tracer one, and hence these results are only a very rough guideline as to the oceanic response to fresh water exchanges. Calculating the response to fresh water involves very intricate details of the surface mixed layer and boundary currents, and is a far more ambitious calculation than is practical at the present time for such long time-spans. Preliminary experiments, not further discussed here, with tracer injected solely within three grid points of the Greenland coast and mimicking ice sheet melt, show very long term confinement to that region, as expected from rotation constraints and comparatively weak lateral diffusion.)

Fig. 10 depicts t_{90} at 1975 m. As expected, an injection confined to the northern North Atlantic requires far longer to bring the remote ocean to equilibrium than does the global input. Estimated t_{90} values for the deep North Pacific are in excess of 7000 years with the Southern Ocean having values between 2000 and 5000 years.
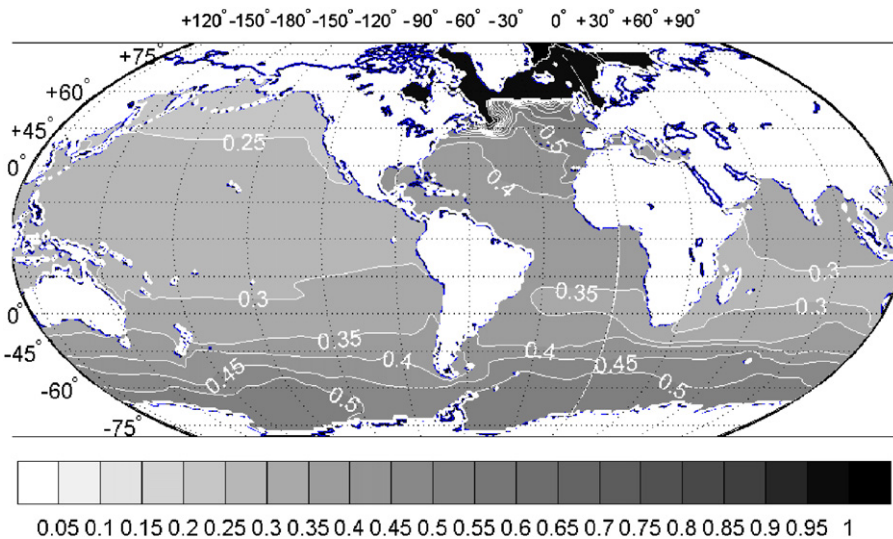
Fig. 9. Tracer concentration at the end of 2000 years at 5 m (middle of the model top layer) from an injection confined to the high latitude North Atlantic. The visually sharp boundary remaining at the southern edge of the injection region exists because of the comparatively weak diffusion and strong northward advection at the sea surface preventing major penetration of the tracer to the south. North Pacific values remain very low.
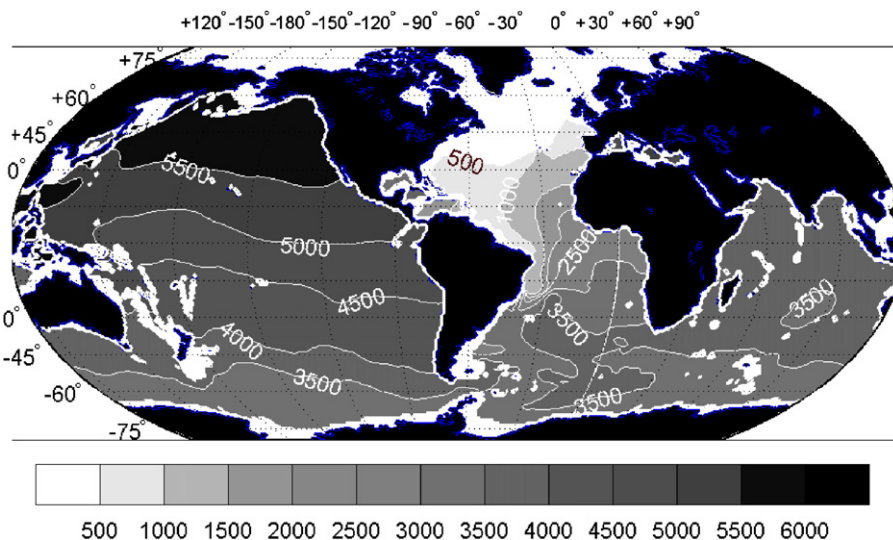

Fig. 10. Value of t_{90} at 1975 m for the high latitude North Atlantic (Fig. 1) injection experiment. As before, any values beyond 2000 years are extrapolations and will underestimate the true value. The model has numerical difficulties near the Rio Grande Rise and the anomalous area east of Brazil is one where the concentration is rising very slowly and the extrapolation is unduly influenced by the short-time scale noise. For this computation, the concentrations were smoothed over 500 years prior to extrapolation. Because of the limited area of injection, t_{90} exceeds, sometimes greatly, the values in the global input experiment.

Within the North Atlantic itself, hundreds of years are required to achieve local equilibrium at depth (not shown, but see Wunsch, 2003). Although this time scale is much shorter than required globally, it can still be significant in the analysis of core data spread over the North Atlantic Basin.

3.3. Southern Ocean injection

The Southern Ocean is also a region where ice-melt would be significant and where there is convection of properties to great depths. Results depend upon which sector of the Southern Ocean is the source region. As one example, Figs. 11 and 12 show the tracer concentrations at the end of the calculation at 15 and 1975 m for Atlantic sector input. Dye is carried rapidly into the North Atlantic where it is convected to large depths, exhibiting a time history not unlike that for North Atlantic injection, except significantly delayed. t_{90} values for the *surface* North Pacific exceed 3000 years everywhere and are about 1000 years for the surface North Atlantic (not shown). At 1975 m, t_{90} exceeds 2000 years in the North Atlantic and is well above 3000 years at the same depth in the Pacific.
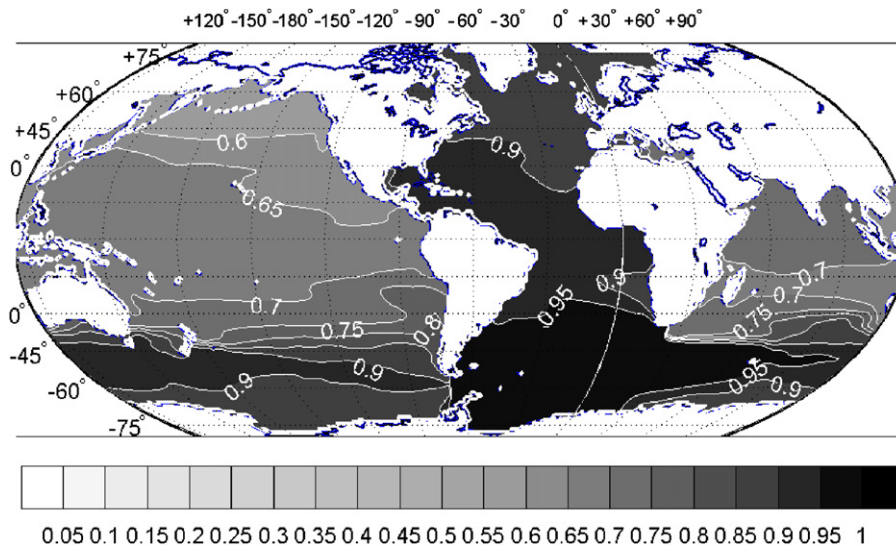
Fig. 11. Tracer concentration at 15 m after 2000 years when injection is confined to the Atlantic sector of the Southern Ocean (see Fig. 1). The dye is swept into the North Atlantic so that subsequent behavior is not unlike the results for direct North Atlantic injection.
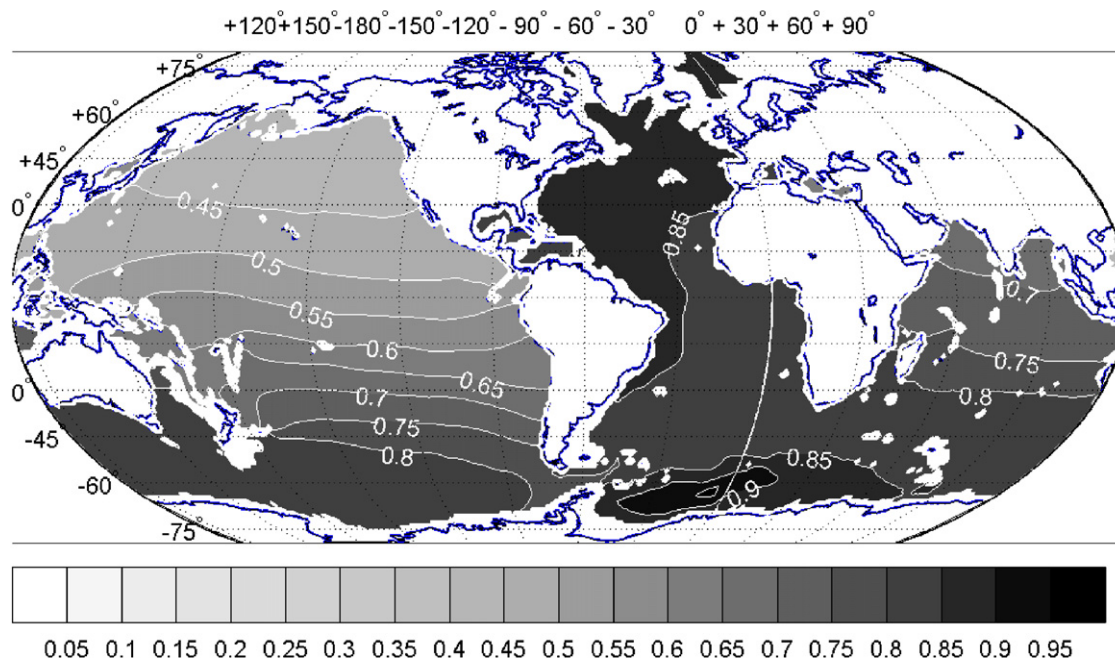

Fig. 12. Tracer concentration after 1900 years at 1975 m in the experiment with injection confined to the Atlantic sector of the Southern Ocean.

When tracer injection is confined to the Pacific sector of the Southern Ocean, there is more rapid penetration of the dye into the North Pacific, but the gross pattern remains somewhat similar to that from injection in the Atlantic sector. Dyed surface fluid moves into the North Atlantic where it subsequently convects and returns to the abyssal Pacific Ocean after a considerable delay—estimated t_{90} exceeding 4000 years in some places.

The important role of North Atlantic convection means that many signals originating far from that ocean will produce strong surface, intermediate, and abyssal onset signals there, and which might easily be erroneously inferred to imply a North Atlantic origin.

3.4. Remaining areas

Although a great many results (available from the authors) exist for the remaining experiments, we confine ourselves here to the experiment with injection restricted to the North Pacific Ocean alone, and Fig. 13 displays the 15 m concentration after 1900 years. Tracer is found everywhere, but the movement into the Indian Ocean
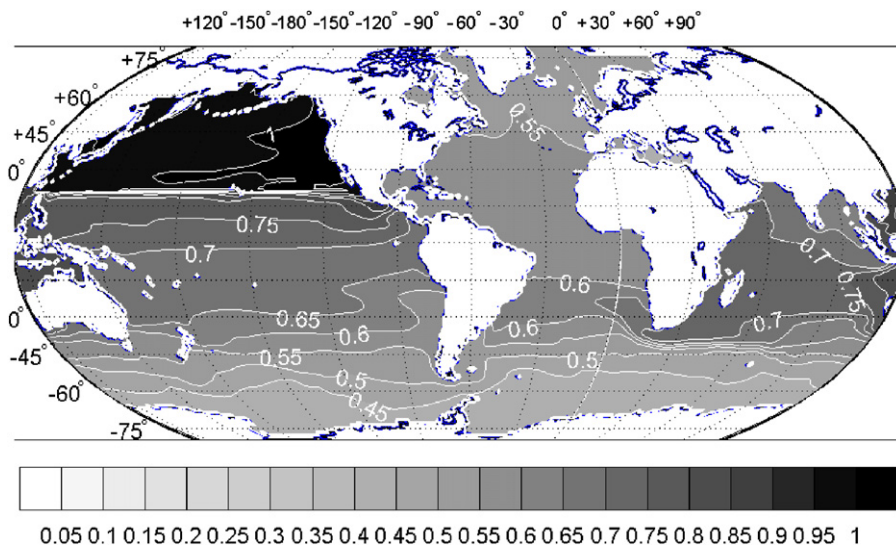
Fig. 13. Tracer concentration at 15 m at the end time from injection in the North Pacific. A complex pattern of surface concentration emerges, although most of the abyssal tracer (not shown) is still injected primarily in the northern North Atlantic.
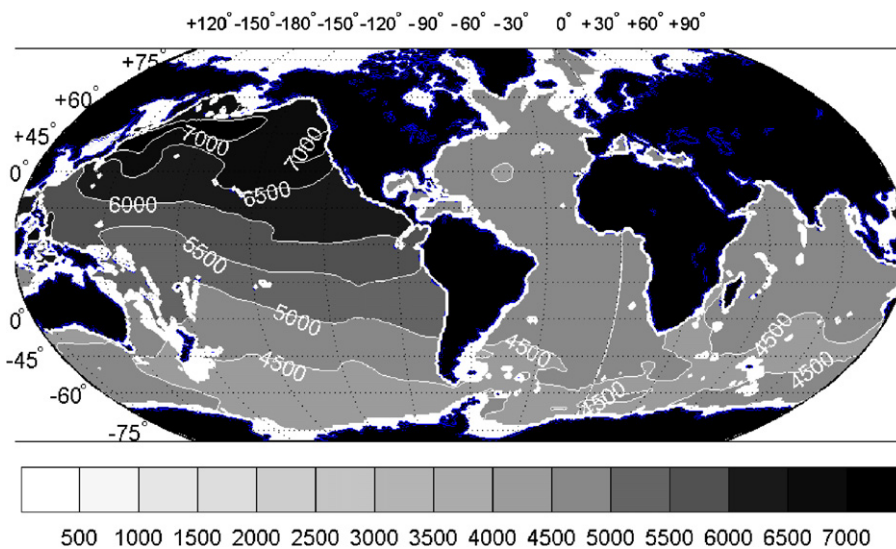

Fig. 14. The t_{90} at 1975 m from the North Pacific injection experiment. Times remain much longer in the abyssal Pacific than in the Atlantic, despite the surface North Pacific injection.

through the Indonesian Passages is perhaps most striking. In the abyssal distribution, most of the dye enters through North Atlantic convection, albeit equilibrium times are greatly extended (Fig. 14), and difficult to estimate from a less than 2000-year calculation.

Note that in the modern world, there is a significant Arctic Basin connection (flows of order 1 Sv) between the North Pacific and North Atlantic, providing a pathway that could "short-circuit" the transfer from the surface North Pacific into a deep convection region—and thus shortening the long equilibrium times found here. Although later versions of the model do include the Arctic, the present one does not. On the other hand, during the Last Glacial Maximum, with lowered sea level, no such pathway exists and the calculations here may be reasonably

accurate. This complication is only one of many that need to be addressed when interpreting real paleo-data.

4. Discussion

No model ever gives the "right" result, and although many details in the results are dependent upon the particular model and the configuration used here, several inferences can be drawn about the interpretation of paleoceanographic data that are likely robust. The present results can be understood as a scale analysis showing the existence in the ocean of memories of past conditions extending as far back as 10,000 years. The ocean displays important non-uniform passive tracer distributions on very long time scales—a result consistent with the more

complete (but more elaborate) transit-time calculations by Peacock and Maltrud (2006) and others. Even where a tracer is globally uniformly distributed at the sea surface (as in transfers from a well-mixed atmosphere), strong vertical and horizontal gradients in concentration remain even after 2000 years, with the North Atlantic closest to uniformity in three-space dimensions, and with the mid-depth North Pacific furthest away. Zonal gradients persist for long times even in the Southern Ocean. For the regional tracer injection, communication with the abyss has to wait until high latitude North Atlantic concentrations are significant. As is conventional wisdom, the deep and intermediate depth North Pacific are the "end-of-the-line." The complementary inference is that the time required to transfer fluid from the deep North Pacific back to the high latitude Southern Ocean or North Atlantic convective region will be extremely long. Tracer differences between the abyssal North Atlantic and North Pacific are among the largest and most persistent in the model world ocean and observed delays of order 4000 years from a nearly fixed modern circulation are consistent with present results. Regional changes in circulation are unnecessary to explain such features but, of course, not precluded. Shifts in surface boundary conditions, be they concentrations as here, or fluxes, will exhibit complex structures through time and space, and will be recorded as such in the sediments.

Because the model North Atlantic has such a strong role in carrying properties from the surface to intermediate and abyssal waters, tracers originating at the sea surface elsewhere (e.g., the North Pacific) can leave signatures appearing to imply, erroneously, a North Atlantic origin. This possibility must be borne in mind when interpreting core data which are sparse in space. There must be particular concern about the so-called glacio-eustatic corrections made to core data, and intended to remove the effects of ice volume changes on deep values of $\delta^{18}O$. As commonly implemented, the glacio-eustatic change is meant to be globally nearly instantaneous (e.g., as in Skinner and Shackleton, 2005). Because melting ice (or evaporating sea water) is introduced at the sea surface, and with a strong regional confinement, such shifts will be subject to precisely the same long transitions to equilibrium seen in the results here. Some regional injection t_{90} values exceed 10,000 years. Evaporation and melting ice have such different spatial distributions, one anticipates important asymmetries in the oceanic spatial distributions of $\delta^{18}O$ as ice-sheets build and decay—they will have to be modelled.

As very briefly described in Appendix B, there is no simple relationship between tracer ages (viz., radiocarbon) and the time to equilibrium or uniformity. In particular, tracer ages depend, among other properties, upon the decay constant of the tracer, are not an intrinsic property of the circulation, and must be interpreted very cautiously. Some values of t_{90} in the present calculations are much longer than estimated radiocarbon ages which potentially have useful interpretations, but cannot be used to claim very short time scales for removal of tracer gradients.

Similarly, reservoir ages produce rough orders of magnitude for change times, but do not describe the very large deviations that can occur regionally within the fluid. The reader is also reminded that times to equilibrium are not the same as signal propagation times. If the solutions here are differentiated in time to give the impulse response, and convolved with temporal transients over the same regions of input, one can compute the response to arbitrary surface tracer transients. In practice, the inability to run the model out closer to true equilibrium means that we do not yet have an adequate time history to fully calculate the impulse response.

That the ocean circulation would remain unchanged over 2000 years and longer times is very implausible. In combination with the inference that the model produces high latitude convection that penetrates too deeply on average, the time scales defined here are likely lower bounds on the true ones. Variations in the flow field or the surface boundary conditions normally will delay the approach to equilibrium. In the present state of under-standing, the results of a 1° horizontal, 23-layer vertical resolution should be regarded as in the spirit of geophysical fluid dynamics, in which major elements of the problem are described, but detailed realism is not intended. The ECCO-GODAE version 2.216 solution, using also a 13-year rather than a 50-year cycling of the meteorological forcing, and used for the same dye experiments over 1300 years produces solutions qualitatively the same as those we have described here, albeit the dye concentrations at depth are generally slightly *smaller* than those focussed on here, and consistent with the inference that we have found lower bounds on the time to homogeneity. But all model solutions are the result of various approximations. In general, eddy and general mixing parameterizations in all models remain the subject of great debate, boundary currents are inadequately resolved at 1° lateral resolution, the Arctic is missing here, sea ice and its effects on salinity and temperature are incompletely represented, the surface boundary condition for fresh water has been linearized, and the mixed layer inadequately described. Taken altogether, however, it seems unlikely that the orders of magnitude estimated could be very wrong. Improper representation of the very localized bottom water formation process around Antarctica remains a particular concern in all existing circulation models.

Anyone seeking a conservative approach to under-standing climate needs to treat the global ocean as being in a transient state for time scales of several thousand years, approaching 10,000 years for regionally injected tracers, unless and until hard evidence emerges showing much more rapid adjustment. Specific regions may well approach uniformity more quickly, but the accuracy of an assumption of a steady-state would be dependent upon details of the interaction with the rest of the ocean. Significant spatial gradients remain in the system for long periods. Even with a circulation in a steady-state, and surface tracer concentrations held fixed in time after onset,

proxy and tracer signatures are likely to display complex space-time gradients except on time scales long compared to 10,000 years and the study of past oceanic circulations requires modelling this transient behavior.

Studies such as this one can be extended in several directions, including the determination of distributions of tracers whose injection varies in time on intervals comparable to or shorter than t_{90}, and to the computation of dynamically active components. Dynamical tracers could conceivably have shorter equilibrium times, but that would have to be demonstrated. Sufficiently small perturbations in salinity or temperature can be expected to exhibit behavior similar to that found for the passive tracers. Some of the phase lags in atmospheric temperatures around the world attributed to changing ocean dynamics may well be nothing but the expected behavior of anomalies that must circulate through three-dimensional ocean pathways before reaching equilibrium. Because ocean surface values reflect at least in part upwelled and diffused fluid coming from below, but originating far away in space and time, one needs to be cautious about attribution. For example, the time scales for apparent leads and lags for temperature and ice volume change discussed, e.g., by Lea (2001), overlap those obtained here and the signal transmission times involving the ocean need to be evaluated.

Appendix A. Version 3 circulation

The circulation used here differs from that discussed by Wunsch and Heimbach (2007) in four major ways: (1) forcing by the atmosphere uses the bulk formulae of Large and Pond (1982) in terms of the atmospheric state variables; (2) consequently, the optimization adjusts the surface atmospheric state, and the adjoint of the bulk formula code provides a physical link between buoyancy and momentum fluxes; (3) the ocean is coupled to the thermodynamic sea-ice model of Parkinson and Washington (1979) as adapted to the MITgcm by Zhang et al. (1998); (4) the parameterization scheme of Bryan and Lewis (1979) is used to enhance vertical mixing near the bottom. After 50 iterations of optimization, the misfits to most observational elements were reduced to values similar to the previously published solution v2.216 of Wunsch and Heimbach (2007), and the solution of this experimental

version 3, labeled v3.50e, deemed useful for the present study. Details of the version 3.n solutions will be provided elsewhere.

Two options were available to use the 13-year state estimate in a millennial-time tracer calculation: (A) offline calculation of the tracer advection/diffusion based on the flow field from the 13-year estimate saved at certain (daily, monthly, or yearly) intervals and used in a perpetual loop and (B) online calculation of the full GCM in a perpetual loop. Because daily output of the full numerical state estimate and mixing tensor fields required for offline calculation is disk-intensive—a resource which was not available at the time of inception—but is important for the representation of intermittent events of deep convection and mixed-layer deepening, we opted for approach (B). Furthermore, two intrinsic loop frequencies were considered: (a) the 13-year period encompassing the state estimate; (b) the 50-year period of the NCEP/NCAR reanalysis (Kalnay et al., 1996). To include as much as possible low-frequency atmospheric variability we opted for (b), but taking advantage of the adjusted atmospheric state over the 13-year period in the following way: climatological monthly (Jan, ..., Dec) mean fields were computed for each adjusted variable (surface air temperature, specific humidity, precipitation, net shortwave radiation, zonal and meridional surface wind speed), recognizing that adjusted patterns recur on a seasonal basis, are reasonably well captured by their monthly mean field, and thus produce corresponding improvements in the misfit of the model to the observations. The model is then run in a perpetual loop, starting over again every 50 years for (at the time of writing) 1950 years, and forced by 6-hourly NCEP/NCAR atmospheric state fields onto which are superimposed the monthly mean ECCO-GODAE adjustments derived from v3.50.

Appendix B. Analytical solutions and ages

B.1. One-dimensional transient

Eq. (18) of Wunsch (2002) has many misprints, and we take the opportunity to both correct it, and to display a qualitatively useful analytical solution. Consider a one-dimensional advection diffusion version of Eq. (1),

$$\frac{\partial C}{\partial t} + w\frac{\partial C}{\partial z} - \kappa\frac{\partial^2 C}{\partial z^2} = 0, \qquad (B.1)$$

in conventional notation subject to a step-boundary condition, $C(z = 0, t) = H(t)$ where $H(t)$ is the Heaviside function. One infers from Carslaw and Jaeger (1986, Appendix V, formula (19)) or Lee (1999, Eq. (7.21), setting his decay constant, $\lambda = 0$) for $z < 0, t \geqslant 0, w > 0$:

$$C(z, t) = \frac{\exp(wz/2\kappa)}{2}\{\exp(wz/2\kappa)\text{erfc}[(-z - wt)/\sqrt{4\kappa t}]$$
$$+ \exp(-wz/2\kappa)\text{erfc}[(-z + wt)/\sqrt{4\kappa t}]\}. \qquad (B.2)$$

This solution represents upwelling of zero dye-concentration fluid toward a surface from which dye is diffusing

downward forming a boundary layer, as depicted in Fig. 15.

If $w < 0$, dye is carried downward, with advection reinforcing diffusion, and the solution is given by Lee's (1999, Eq. (7.21)) with the substitution $x \rightarrow -z$, represents a moving front. Some regions of the three-dimensional ocean may display transient tracer characteristics somewhat like these oversimplified one-dimensional solutions, but their use must be purely qualitative. In a closed system such as the one focussed on in the main text, the boundary layer solution can apply only for finite time, as no infinite reservoir of dye-free fluid is available for indefinite periods.

B.2. One-dimensional steady-state ages

For some insight into the behavior of conventionally defined "ages", e.g., for ^{14}C, consider the steady-form of Eq. (B.1), for a decaying tracer:

$$w \frac{\partial C}{\partial z} - K \frac{\partial^2 C}{\partial z^2} = -\lambda C.$$

Then if the tracer is held at a surface value of $C(z = 0) = C_0$, and with $w > 0$ (so that the balance is that of the abyssal-Munk type), then

$$C = C_0 \exp\left(\left[\frac{w}{2K} + \frac{1}{2}\left(\frac{w^2}{K^2} + \frac{4\lambda}{K} \right)^{1/2} \right] z \right) \quad (B.3)$$

with a surface boundary layer character. Defining the age relative to the assumed (here fixed) surface value, as usually done for ^{14}C:

$$\tau = -\frac{1}{\lambda} \ln\left(\frac{C(t)}{C_0} \right) = -\left(\left[\frac{w}{2K} + \frac{1}{2}\left(\frac{w^2}{K^2} + \frac{4\lambda}{K} \right)^{1/2} \right] z \right) \Big/ \lambda. \quad (B.4)$$

Then Fig. 16 displays the concentration and apparent age at $z = -1000$ m as a function of λ (in this particular case, age is a linear function of depth). The main point is that the age varies by orders of magnitude with λ, and thus has no simple physical interpretation. Fluid upwelling from the abyss is tracer-free in this situation, with a formally infinite age. The finite ages found near the surface are solely due to the downward diffusion of tracer from the high concentration region at the surface and no connection to a travel time from the surface is available. It may be confirmed, that an age based upon a parent/daughter ratio, as is used commonly for the tritium/helium pair, is also dependent upon λ, and differs significantly from τ with all other variables fixed. Distributions in time-varying three-dimensional flows are much more complex than for a one-dimensional steady-state and interpretation of any computable age as a time since a fluid parcel (in the Lagrangian sense) was at the surface would have to be very carefully justified.
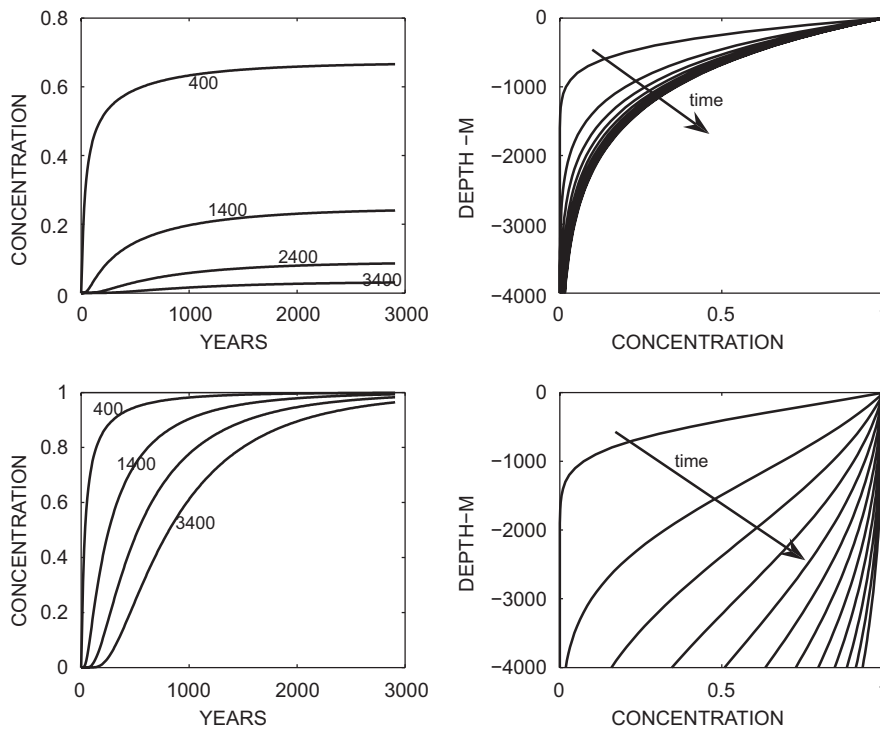

Fig. 15. One-dimensional analytical transient solutions. In the upper two panels, dye-free fluid is upwelling toward a surface from which dye is diffusing downwards so that a boundary-layer forms. In the left panel, time histories at four depths (meters) are shown and in the right panel depth profiles with increasing time are displayed. $\kappa = 10^{-4}$ m^2/s, $w = 10^{-7}$ m/s, and the dimensional time history is over 3000 years at intervals of 25 years. Lower two panels show the contrasting situation in which the fluid is downwelling from the surface so that dye is carried into the abyss as a moving, diffusive front. Numerical values are the same as in the upper panels.
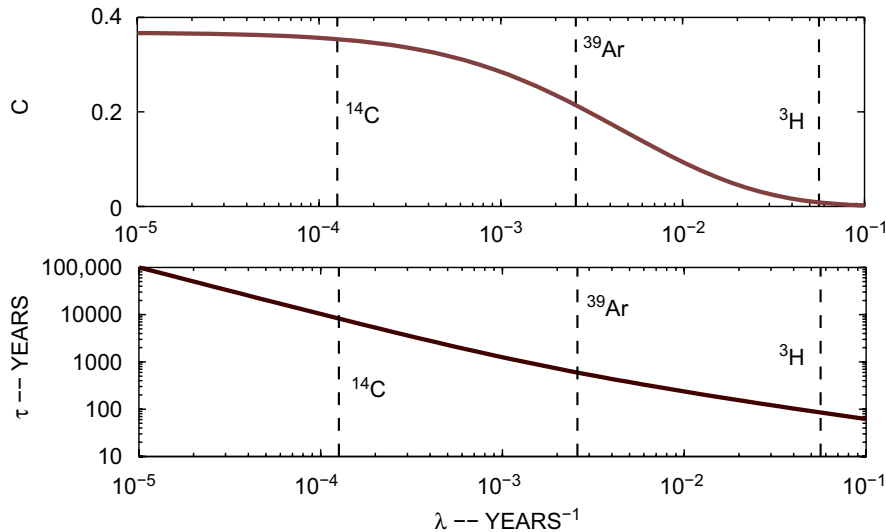
Fig. 16. Dependence of a "radiocarbon" age on the decay constant of the tracer. Upper panel displays the concentration, C, at $z = -1000\,\mathrm{m}$ as a function of the decay constant of the tracer. Generic tracer, C, should not be confused with radiocarbon concentration. Lower panel shows the apparent "age" and its dependence upon λ—the strong dependence shows conspicuously that the age is a property of the tracer, not so much of the fluid flow. The values of λ appropriate for ^{14}C, ^{39}Ar, and ^{3}H are shown as vertical dashed lines.

B.3. Tracer ages in the small λ limit

Tracer ages can be used to test general circulation models (e.g., England, 1995), but so can the tracer distribution itself (England and Maier-Reimer, 2001), without the intermediate complication of an age equation, although in both cases, observations are always uncertain, sometimes to a large degree. In a GCM, a decaying tracer will satisfy an equation such as

$$\frac{\partial C}{\partial t} + \mathbf{v} \cdot \nabla C - \nabla(\mathbf{K}\nabla C) = -\lambda C, \qquad (B.5)$$

which is the same is Eq. (1), except for the introduction again of the decay term. One requires $\nabla \cdot \mathbf{v} = 0$, with appropriate initial and boundary conditions on C. A reviewer claims that as λ becomes very small, the ordinary tracer age becomes independent of λ. Or, more formally, that

$$\frac{\partial}{\partial \lambda}\left[\lim_{\substack{\lambda \to 0 \\ t \to \infty}} \frac{1}{\lambda} \ln\left(\frac{C(\mathbf{r}, t)}{C_0(\mathbf{r})}\right)\right] = 0,$$

explicitly accommodating spatial variation in the surface boundary conditions in the steady-state. This conjecture about the solutions of Eq. (B.5) is an interesting one, and potentially important for age distributions in turbulent fluids—if it is correct. No proof is known to us and Eq. (B.4) is a counter-example, with a strong dependence on λ as $\lambda \to 0$, albeit in an open one-dimensional domain. If the radiocarbon or other age is demonstrably independent of λ, one would recover a property that is once again dependent only on the fluid physics and not that of the tracer. Interpretation as an age would still have to be done as, e.g., in the transit-time distributions. Similar conjectures can be made concerning ages from parent/daughter pairs, but they again remain speculation.

References

Bryan, K., Lewis, L.J., 1979. A water mass model for the world ocean. Journal of Geophysical Research 84, 2503–2517.

Carslaw, H.S., Jaeger, J.C., 1986. Conduction of Heat in Solids. Oxford University Press, Oxford, 510pp.

Duplessy, J.C., Bard, E., Arnold, M., Shackleton, N.J., Duprat, J., Labeyrie, L., 1991. How fast did the ocean-atmosphere system run during the last deglaciation. Earth Planetary Science Letters 103, 27–40.

England, M.H., 1995. The age of water and ventilation timescales in a global ocean model. Journal of Physical Oceanography 25, 2756–2777.

England, M.H., Maier-Reimer, E., 2001. Using chemical tracers to assess ocean models. Reviews of Geophysics 39, 29–70.

Gent, P.R., McWilliams, J.C., 1990. Isopycnal mixing in ocean circulation models. Journal of Physical Oceanography 20, 150–155.

Haine, T.W.N., Hall, T.M., 2002. A generalized transport theory: water mass composition and age. Journal of Physical Oceanography 32, 1932–1946.

Huang, R.X., 1999. Mixing and energetics of the oceanic thermohaline circulation. Journal of Physical Oceanography 29, 727–746.

Kalnay, E., et al., 1996. The NCEP/NCAR 40-year reanalysis project. Bulletin of the American Meteorological Society 77, 437–471.

Key, R.M., Kozyr, A., Sabine, C.L., Lee, K., Wanninkhof, R., Bullister, J.L., Feely, R.A., Millero, F.J., Mordy, C., Peng, T.H., 2004. A global ocean carbon climatology: results from Global Data Analysis Project (GLODAP). Global Biogeochemical Cycles 18, Art. No. GB4031, doi:4010.1029/2004GB002247.

Khatiwala, S., Visbeck, M., Cane, M.A., 2005. Accelerated simulation of passive tracers in ocean circulation models. Ocean Modelling 9, 51–69.

Large, W.G., Pond, S., 1982. Sensible and latent-heat flux measurements over the ocean. Journal of Physical Oceanography 12, 464–482.

Large, W.G., McWilliams, J.C., Doney, S.C., 1994. Oceanic vertical mixing: a review and a model with nonlocal boundary layer parameters. Reviews of Geophysics 32, 363–403.

Lea, D.W., 2001. Ice ages, the California Current, and Devils Hole. Science 293, 59–60.

Lee, T.-C., 1999. Applied Mathematics in Hydrogeology. Lewis Publishers, Boca Raton, 382pp.

Marshall, J., Adcroft, A., Hill, C., Perelman, L., Helsey, C., 1997. A finite-volume, incompressible Navier–Stokes model for studies of the ocean on parallel computers. Journal of Geophysical Research 102, 5753–5766.

Parkinson, C.L., Washington, W.M., 1979. Large-scale numerical-model of sea ice. Journal of Geophysical Research 84, 311–337.

Peacock, S., Maltrud, M., 2006. Transit-time distributions in a global ocean model. Journal of Physical Oceanography 36, 474–495.

Primeau, F.W., Holzer, M., 2006. The ocean's memory of the atmosphere: residence-time and ventilation-rate distributions of water masses. Journal of Physical Oceanography 36, 1439–1456.

Sarmiento, J.L., Gruber, N., 2006. Global Biogeochemical Dynamics. Princeton, 503pp.

Skinner, L.C., Shackleton, N.J., 2005. An Atlantic lead over Pacific deep-water change across termination I: implications for the application of the marine isotope state stratigraphy. Quaternary Science Reviews 24, 571–580.

Waugh, D.W., Hall, T.M., Haine, T.W.N., 2003. Relationships among tracer ages. Journal of Geophysical Research 108 (C5) Art. No. 3138.

Wunsch, C., 2002. Oceanic age and transient tracers. Analytical and numerical solutions. Journal of Geophysical Research 107 (C6) DOI:10.1029/2001JC000797, 1–1 to 1–16.

Wunsch, C., 2003. Determining paleoceanographic circulations, with emphasis on the Last Glacial Maximum. Quaternary Science Reviews 22 (2–4), 371–385.

Wunsch, C., Heimbach, P., 2006. Decadal changes in the North Atlantic meridional overturning and heat flux. Journal of Physical Oceanography 36, 2012–2024.

Wunsch, C., Heimbach, P., 2007. Practical global oceanic state estimation. Physica D 230, 197–208.

Zhang, J., Hibler, W.D., Steele, M., Rothrock, D.A., 1998. Arctic ice-ocean modeling with and without climate restoring. Journal of Physical Oceanography 28, 191–217.